Design considerations for a contactless electric vehicle battery charger

Chwei-Sen Wang* Oskar H. Stielau†

Grant Covic‡

*University of Auckland,

†University of Auckland,

‡University of Auckland, g.covic@auckland.ac.nz

Design Considerations for a Contactless Electric Vehicle Battery Charger

Chwei-Sen Wang, Oskar H. Stielau, and Grant A. Covic, *Senior Member, IEEE*

***Abstract*—This paper overviews theoretical and practical design issues related to inductive power transfer systems and verifies the developed theory using a practical electric vehicle battery charger. The design focuses on the necessary approaches to ensure power transfer over the complete operating range of the system. As such, a new approach to the design of the primary resonant circuit is proposed, whereby deviations from design expectations due to phase or frequency shift are minimized. Of particular interest are systems that are neither loosely nor tightly coupled. The developed solution depends on the selected primary and secondary resonant topologies, the magnetic coupling coefficient, and the secondary quality factor.**

***Index Terms*—Battery charging, electric vehicle, electromagnetic coupling, inductive power transfer, resonance.**

I. Introduction

INDUCTIVELY coupled power transfer (ICPT) systems are designed to deliver power efficiently from a stationary primary source to one or more movable secondary loads over relatively large air gaps via magnetic coupling. The fundamental principles of such systems are identical to well known closely coupled electromechanical devices such as transformers and induction motors, where the leakage inductance is much lower than the mutual inductance.

The mutual coupling within ICPT systems is generally weak. To deliver the required power and ensure equipment sizes remain manageable, it is necessary to operate at high frequency (normally above the audible range). At present, the operational frequency for high power applications is limited to below 100 kHz as a result of switching losses. Moreover, resonant circuits are normally employed in the primary and/or secondary networks to further boost the power transfer capability, while minimizing the required voltage and current ratings of the power supply.

Modern power electronics have enabled many new applications such as contactless power supply for professional tools [1], contact-less battery charging across large air gaps for electric vehicles [2], compact electronic devices [3], mobile phones [4], and medical implants [5]. Other examples include material handling systems [6], [7] and public transport systems [8] where the secondary systems are electrically isolated and move along a long track. Electric isolation is also essential for power supplies in harsh environments such as mining and outdoor lighting. The advantages of such systems are safety, reliability, low maintenance, and long product life.

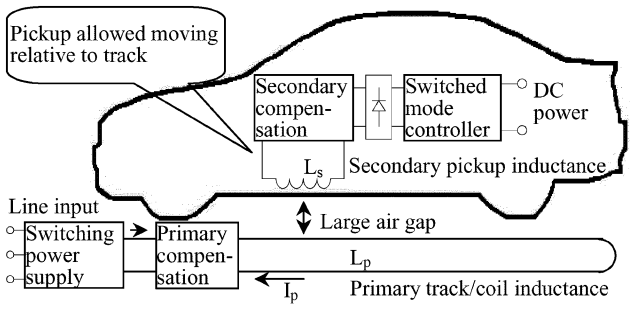

Fig. 1. Structure of inductive power transfer system.

Both the primary and secondary resonant circuits of the ICPT systems are normally designed to operate at the nominal resonant frequency, but care must be taken in such designs since system performance could deviate from design expectations if the loading becomes significant. Generally, such deviations are small if the mutual inductance is much lower than the leakage inductance, but become more significant if the mutual inductance is comparable to the leakage inductance as is the case in many practical applications. In this paper, a general design approach is proposed that includes the magnetic coupling effect in the primary resonance design for the commonly used resonant topologies. A design example for contactless electric vehicle battery charging using a variable-frequency controller is proposed and verified.

II. Fundamental Analysis

A. Fundamental Structure

An ICPT system essentially is comprised of two magnetically coupled electrical systems, as shown in Fig. 1, driven by a high-frequency switching power supply. The primary winding (stationary track or coil) is normally compensated in order to minimize the VA rating of the supply. Compensation is often required for the secondary winding (movable pickup) to enhance the power transfer capability. A switched-mode controller may be used to control the power flow from the pickup to the load. In more complex systems many individual pickups can exist, supplied by a single track.

Manuscript received December 11, 2002; revised April 2, 2004. Abstract published on the Internet July 15, 2005. This work was supported in part by the Foundation of Research, Science and Technology (FRST), New Zealand.

C.-S. Wang and G. A. Covic are with the Department of Electrical and Computer Engineering, The University of Auckland, Auckland 1001, New Zealand (e-mail: ga.covic@auckland.ac.nz).

O. H. Stielau was with the Department of Electrical and Electronic Engineering, The University of Auckland, Auckland, New Zealand. He is now at 152B Forrest Hill Road, Forrest Hill, Auckland 1309, New Zealand.

Digital Object Identifier 10.1109/TIE.2005.855672

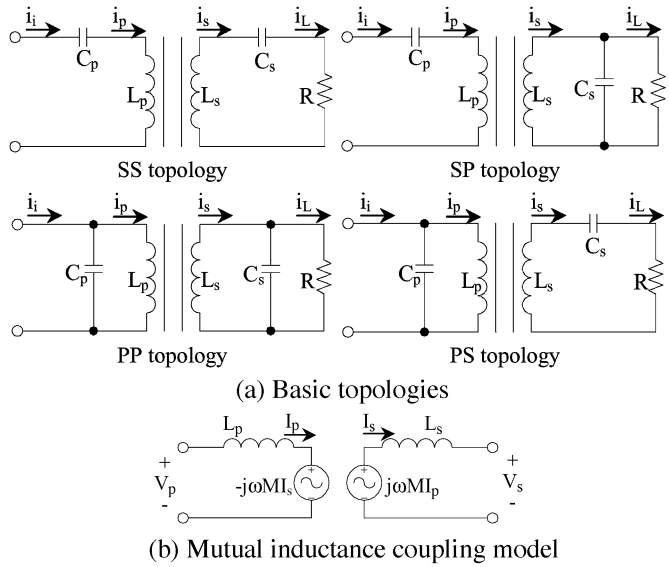

Fig. 2. (a) Basic topologies. (b) Mutual inductance coupling model.

B. Basic Topologies

Four basic topologies labeled as SS, SP, PP, and PS are shown in Fig. 2(a), where the first S or P stands for series or parallel compensation of the primary winding and the second S or P stands for series or parallel compensation of the secondary winding. Here, the subscripts "i", "p", "s", and "L" stand for "inverter", "primary", "secondary", and "load", respectively. The resistance R represents the load on the secondary. Using a mutual inductance coupling model, each of these topologies can be modeled by the circuit shown in Fig. 2(b) for sinusoidal steady state analysis. The induced and reflected voltages in this model are specified in terms of the mutual inductance "M", the operational frequency "ω", and the primary and secondary currents. The mutual inductance is related to the magnetic coupling coefficient by

$$k = \frac{M}{\sqrt{L_p L_s}}. \tag{1}$$

C. Single Pickup

The reflected impedance from the secondary to the primary can be found by dividing the reflected voltage by the primary current resulting in

$$Z_r = \frac{\omega^2 M^2}{Z_s} \tag{2}$$

where Z_s is the impedance of the secondary network and depends on the selected compensation topology.

The power transferred from the primary to the secondary is the reflected resistance multiplied by the square of primary current as given by

$$P = (\mathrm{Re} Z_r) I_p^2 \tag{3}$$

where the operator "Re" represents the real component of corresponding variable.

TABLE I
SECONDARY IMPEDANCE, LOAD VOLTAGE/CURRENT, AND PROPERTIES AT THE SECONDARY RESONANT FREQUENCY. (a) SECONDARY IMPEDANCE AND LOAD VOLTAGE/CURRENT. (b) PROPERTIES AT THE SECONDARY RESONANT FREQUENCY ω_0

(a)

Compensation	Series	Parallel
Secondary impedance Z_s	$j\omega L_s + \frac{1}{j\omega C_s} + R$	$j\omega L_s + \frac{1}{j\omega C_s + \frac{1}{R}}$
Load voltage V_L	$I_s R$	V_s
Load current I_L	I_s	$\frac{V_s}{R}$

(b)

Compensation	Series	Parallel
Reflected resistance	$\frac{\omega_0^2 M^2}{R}$	$\frac{M^2 R}{L_s^2}$
Reflected reactance	0	$-\frac{\omega_0 M^2}{L_s}$
Secondary Quality factor Q_s	$\frac{\omega_0 L_s}{R}$	$\frac{R}{\omega_0 L_s}$

The current flowing through the secondary winding is

$$I_s = \frac{j\omega M I_p}{Z_s}. \tag{4}$$

The voltages across the primary and secondary windings are, therefore, given by

$$V_p = j\omega L_p I_p - j\omega M I_s \tag{5}$$

and

$$V_s = j\omega M I_p - j\omega L_s I_s. \tag{6}$$

The secondary impedance is given in Table I(a) for series- and parallel-compensated networks. The load voltage and current are also given in the same table. Normally, the primary and secondary resonant frequencies are identical as given by

$$\omega_0 = \frac{1}{\sqrt{C_s L_s}} = \frac{1}{\sqrt{C_p L_p}}. \tag{7}$$

The reflected resistance and reactance calculated from (2) at the secondary resonant frequency are also given in Table I(b) and depend on the compensations used. The secondary quality factor defined at the secondary resonant frequency is also given in the same table. Here, the quality factor is the ratio between reactive and real power.

The series-compensated secondary resembles a voltage source, while the parallel-compensated secondary looks like a current source. Both properties can be verified by (3) using the reflected resistance in Table I(b) and assuming that the primary current is maintained constant, which is normally the case in ICPT designs [7], [8]. One of the advantages of a series-compensated secondary is that there is no reflected reactance at the secondary resonant frequency. In contrast, the parallel-compensated secondary reflects a capacitive reactance at the secondary resonant frequency, but this can be tuned out because it is independent of the load.

The load impedance seen by the power supply is determined by combining the primary and secondary networks. For a series-compensated primary system, this load impedance is

$$Z_t = \frac{1}{j\omega C_p} + j\omega L_p + Z_r. \tag{8}$$

For a parallel-compensated primary system, this load impedance is

$$Z_t = \frac{1}{j\omega C_p + \frac{1}{j\omega L_p + Z_r}}. \tag{9}$$

D. Multiple Pickups

With multiple pickup ICPT systems, all pickups are normally designed identically so that secondary impedances are identical for each loading condition. As a result, the total reflected impedance from all pickups is

$$\sum_{i=1}^{n} Z_{ri} = n\frac{\omega^2 M^2}{Z_s} \tag{10}$$

where n is the number of pickups.

This is equivalent to the reflected impedance of a single identical pickup with an equivalent mutual inductance of

$$M_n = \sqrt{n}M. \tag{11}$$

The equivalent coupling coefficient is then

$$k_n = \sqrt{n}k. \tag{12}$$

III. General Design Considerations

A. Operational Frequency

In some applications where frequency is adjusted to regulate power flow, operation above or below the secondary resonant frequency may be preferred in order to improve the controllability [5] because in such applications the relationship between frequency and power has been found to be approximately linear over the operating frequency range. For most applications, however, operation at or near the secondary resonant frequency is a logical choice because maximum power transfer capability can be achieved. Furthermore, it is also desired that the output voltage and current of the power supply be in phase in order to minimize the VA rating of the power supply. This can be achieved by operating at the zero-phase-angle (ZPA) frequency of the load impedance. Consequently, the nominal frequency of the ICPT system is normally designed to achieve primary ZPA operation at the secondary resonant frequency.

B. Control

The power supply and primary controller normally control both the frequency and the primary current to achieve maximum power transfer capability. Both fixed- and variable-frequency controllers can be used. Power flow regulation is also required because of variations in load and other system parameters.

1) Power Flow Regulation: One common approach to achieve power flow regulation is to detune the system by shifting the operational frequency of the power supply. This approach is not suitable for many multiple pickup applications where the load condition on each pickup can be different. Here, detuning the power supply affects all the secondary pickups so that some pickups may be unable to deliver the necessary power. An alternative approach is to use a switched-mode controller within the secondary pickup for power flow control [4], [7], [8]. Using this approach, each pickup can be controlled separately or even decoupled completely from the primary. However, the disadvantages are increased switching losses and a higher cost of the secondary pickups.

2) Fixed-Frequency Control: With fixed-frequency-controlled applications, variations in load and coupling between the primary and secondary will cause a phase shift in the load impedance. If this phase shift is significant, then the power supply must have a higher VA rating for the same power transfer.

3) Variable-Frequency Control: As noted in Section III-A, most variable-frequency controllers operate at the primary ringing frequency. However, the operational frequency (ZPA frequency of the load impedance) will shift away from the nominal resonant frequency because of the variations in the load and the degree of coupling between the primary and secondary. This results in a loss of power transfer capability if the frequency shift is too large, and may also result in a loss of frequency stability and controllability because of the onset of bifurcation with increasing load, where more than one primary ZPA frequency exists [7], [9], [10].

C. Design Procedure

The design of ICPT systems relies strongly on experience and experimental verification because of the complexity regarding the interactions of the primary and secondary resonant circuits. A generalized design methodology is proposed in [9] assuming the system is operated at the nominal resonant frequency. With this iterative design procedure, the electromagnetic structure as well as the primary current can be determined for the required power transfer. The physical limit to the power transfer capability of a proposed electromagnetic coupling structure is its VA rating. In this design process, power transfer capability is assured under the primary and secondary VA ratings.

The selection of the primary and secondary compensation topologies are generally application oriented as described in [9]. A series-compensated secondary can supply a stable voltage, while a parallel-compensated secondary is able to supply a stable current. A series-compensated primary is normally required to reduce the primary voltage to manageable levels for long track applications, whereas a parallel-compensated primary is usually used to give a large primary current.

In the above design procedure, there are two fundamental assumptions. The first is that the operating frequency remains constant at the nominal resonant frequency as determined by (7). The second is that the primary current is constant. However, as described in the above subsection, there could be significant frequency or phase shift with changing load. With a large frequency shift, the assumption of operation about the nominal resonant frequency is not valid. With a large phase shift, the desired constant primary current is not available when the required VA

TABLE II
PRIMARY COMPENSATION

Topology	Primary Capacitance C_p	Normalized Primary Capacitance C_{pn}	Examples C_{pn} Q_s=10		
			k=0.1	k=0.2	k=0.3
SS	$\frac{C_s L_s}{L_p}$	1	1	1	1
SP	$\frac{C_s L_s^2}{L_p L_s - M^2}$	$\frac{1}{1-k^2}$	1.01	1.04	1.10
PP	$\frac{(L_p L_s - M^2) C_s L_s^2}{\frac{M^4 C_s R}{L_s} + (L_p L_s - M^2)^2}$	$\frac{1-k^2}{Q_s^2 k^4 + (1-k^2)^2}$	1.00	0.89	0.56
PS	$\frac{C_s L_s}{\frac{M^4}{L_p C_s L_s R} + L_p}$	$\frac{1}{Q_s^2 k^4 + 1}$	0.99	0.86	0.55

rating exceeds the capability of the selected power supply. In either case, the system will be unable to deliver the required power.

D. Choice of Primary Compensation Capacitance

To minimize the above problems associated with frequency or phase shift, primary ZPA operation at or near the secondary resonant frequency is desired. One simple approach is to select the primary capacitance deliberately by letting the imaginary component of the load impedance equal zero at the secondary resonant frequency. This design approach compensates not only the primary inductance but also the existing reflected impedance in series with the primary winding. The solutions are given in Table II for the four basic topologies in Fig. 2.

For a general analysis, a normalized primary capacitance can be defined as the primary capacitance in Table II divided by the primary capacitance determined by (7). The result is

$$C_{pn} = \frac{C_p}{\frac{C_s L_s}{L_p}}. \tag{13}$$

This normalized primary capacitance is unity when the primary capacitance is determined by (7). According to Table II, the primary capacitance for achieving primary ZPA operation at the secondary resonant frequency depends on three factors: the selected primary and secondary topologies, the magnetic coupling coefficient, and the secondary quality factor.

E. Topology Dependency

As can be seen from the results above, the selected topology plays a large role in the correct choice of the primary capacitance. Since the series-compensated secondary reflects no reactance at the nominal resonant frequency, the primary inductance can be tuned out independent of either the magnetic coupling or the load by a series-connected capacitance in the primary network. As the parallel-compensated secondary reflects a load-independent capacitive reactance at the nominal resonant frequency, series tuning in the primary is dependent on the magnetic coupling but not the load. Because the reflected impedance contains a real component representing the load, parallel tuning in the primary becomes dependent on both the magnetic coupling and the load.

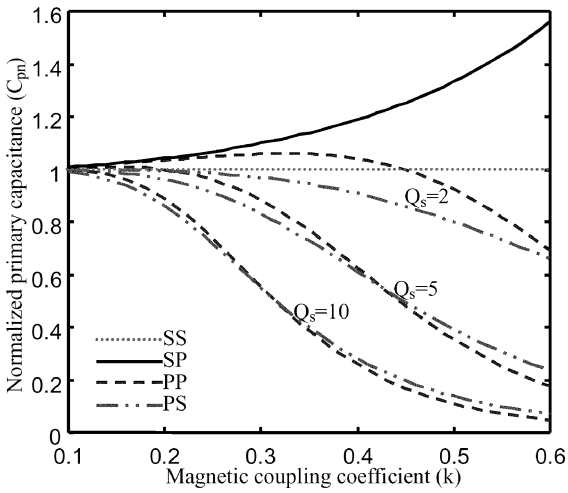

Fig. 3. Normalized primary capacitance.

Theoretically, SS is the best topology, as the primary capacitance is then independent of either the magnetic coupling or the load. The other three topologies are all dependent on the magnetic coupling, while parallel-compensated primaries are a function of the load as well. Although SS topology seems to be the best choice regarding primary resonance design, parallel compensation may be preferred in the primary and/or secondary resonant circuits for many applications [1]–[3], [6]–[8], [10] because of practical considerations as noted in Section III-B.

F. Effects of Coupling and Secondary Quality Factor

As shown above, the magnetic coupling and/or the secondary quality factor (corresponding to the rated load) must be included in the choice of the primary compensation capacitance. In order to investigate the effects of the magnetic coupling and the secondary quality factor on the proposed primary resonance design, the normalized primary capacitance determined by Table II is shown in Fig. 3 as a function of the magnetic coupling coefficient for selected secondary quality factors that range typically from 2 to 10. As shown here, no change from that determined by (7) is required for SS topology. The SP topology requires a larger primary capacitance with better coupling. The PP topology requires a slightly larger primary capacitance for loose coupling with low secondary quality factor, but needs a smaller primary capacitance if the coupling is improved or the secondary quality factor is increased. A smaller primary capacitance is always required for PS topology and the change becomes larger with better coupling or higher secondary quality factor.

To increase the power transfer capability of ICPT systems, much effort has gone into improving the magnetic coupling between the primary and secondary, and coupling coefficients for single pickup applications of between 0.3–0.6 are often achievable [1]–[3], [5], [10]. For multiple pickup applications, system constraints usually result in coupling coefficients of less than 0.1 per pickup [6]–[8], but the effect of all pickups together is often again equivalent to a single pickup with a coupling coefficient of about 0.5.

As can be seen in Fig. 3, systems with such high coupling coefficients behave very differently to traditional loosely coupled systems. For coupling coefficients of less than 0.2, the system can be considered loosely coupled and traditional design approaches as discussed in [9] that use (7) to determine the primary capacitance give good results. However, as the coupling improves the system characteristics change substantially. This change is a strong function of both the system topology as well as the secondary quality factor Q_s. The SS topology does not present a problem, but the other three topologies do. With Q_s equal to 10, PP and PS topologies start deviating from the loosely coupled theory at coupling coefficients exceeding about 0.2, while for lower Q_s values of 2 the deviation only occurs at coupling coefficients exceeding about 0.5.

Examples of the normalized primary capacitance are given in Table II. Here, the design changes of three different coupling coefficients are compared assuming a secondary quality factor of 10. The required primary capacitance is close to that designed by (7) if the coupling coefficient is small. With a coupling coefficient of 0.1, the reflected impedance is negligible and as such affects the primary compensation design by less than 1%. When the coupling coefficient is around 0.2, the design can change by as much as 4% for SP topology, 11% for PP topology, and 14% for PS topology. A coupling coefficient of 0.3 changes the design significantly by 10% for SP topology, 44% for PP topology, and 45% for PS topology.

From the above it can be seen that care needs to be taken when applying the loosely coupled ICPT theory. The traditional design rules work well for the SS topology, and for other topologies with low Q_s (less than 2) or coupling coefficients less than 0.2. Special care needs to be taken when designing system with PP or PS topologies that have good coupling and high Q_s.

IV. Proposed Design Example

A contactless electric vehicle battery charging system was designed to deliver 30 kW across a 45-mm air gap at a nominal frequency of 20 kHz with a primary current I_p of 150 A. The selected magnetic coupling structure is shown in Fig. 4(a). Here, the primary and secondary windings are identical, each having concentrated coils with a magnetic linking path. It is assumed that the secondary coil is attached to the underside of an electric vehicle, while the primary coil is buried in the ground. Once an electric vehicle has stopped over the charging system, electric power is transferred across an air gap via magnetic coupling between the primary coil in the ground and the secondary coil on the vehicle.

The electric circuit schematic is shown in Fig. 4(b). Both the primary and secondary windings are compensated using a parallel-connected capacitor (PP topology in Fig. 2(a)). The current source characteristic of the parallel secondary is suitable for battery charging. The parallel primary is used to generate a large primary current. The parallel-compensated primary winding acts as the resonant tank of the full-bridge inverter fed by a dc voltage V_d. A series inductor L_r is used to regulate the inverter current i_i flowing into the parallel-resonant tank. In order to make the current rating of the inverter as low as possible to achieve minimum cost and maximum efficiency,

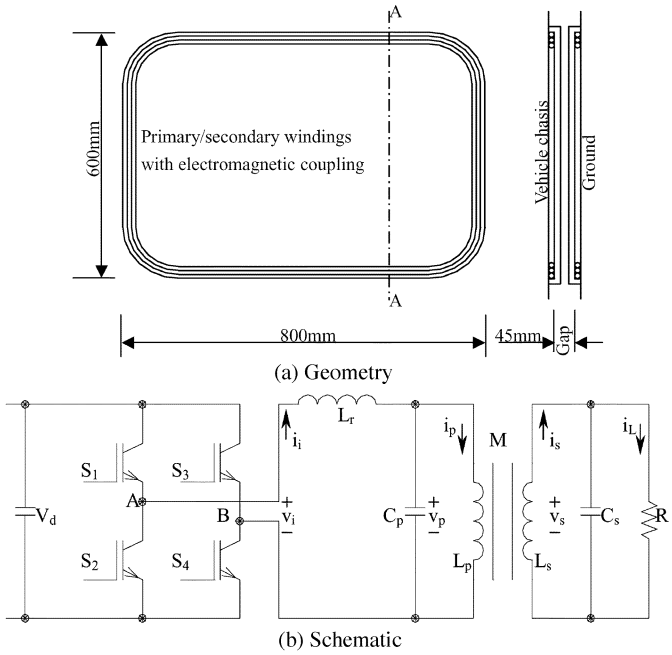

Fig. 4. Selected structure of the contactless electric vehicle battery charger. (a) Geometry. (b) Schematic.

TABLE III
PARAMETERS OF THE CONTACTLESS ELECTRIC VEHICLE BATTERY CHARGER

Nominal frequency	20kHz
Rated power	30kW
Primary rated current	150A
Rated load	6Ω
Primary inductance	29.6μH
Primary capacitance	2.28μF
Mutual inductance	12.7μH
Secondary inductance	26.9μH
Secondary capacitance	2.42μF

the inverter current i_i is controlled to follow the resonant tank voltage v_p using a variable-frequency controller. The system is, therefore, operated at the ringing frequency of the primary resonant tank.

The measured coupling parameters are given in Table III along with other system parameters. The magnetic coupling coefficient is 0.45 and the secondary quality factor is 1.77. According to Table II, the normalized primary capacitance is 1.04 and as such the primary capacitance is selected 4% larger than that determined by (7).

V. Design Verification

As noted above, the inverter current is controlled to be in phase with the resonant tank voltage and as such the operational frequency is identical to the ZPA frequency of the load impedance. This frequency can be calculated from (9) by letting the imaginary component equal zero. The power transferred from the primary to the secondary at each ZPA frequency is then given by (3). The ZPA frequencies and the corresponding power transferred at each operating point are shown in Fig. 5 as functions of the load. As shown, three different ZPA frequencies

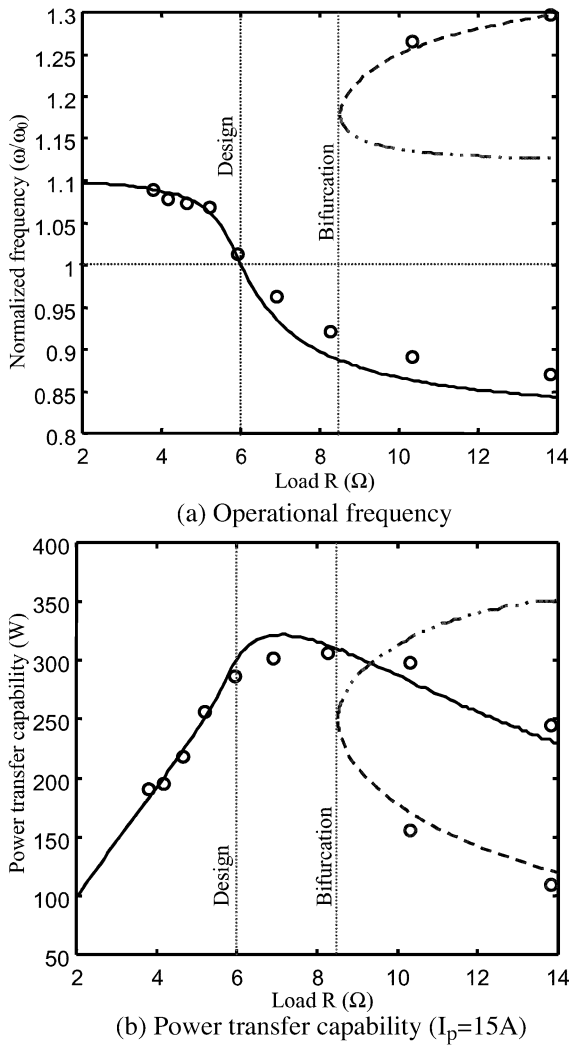

Fig. 5. (a) Operational frequency. (b) Power transfer capability ($I_p = 15$ A).

exist if the load is greater than the normal operating level. This is called the bifurcation region.

In order to compare theory with the experimental results taken in the lab, the primary current was controlled at a relatively low level of 15 A. With this change in primary current, all the system characteristics are identical except that the power level is scaled down by one hundredth. The measured operational frequencies and power transfers are shown as circles at selected loads.

As shown in Fig. 5(a), operation at the nominal frequency is achieved at rated load, and bifurcation is only apparent at higher loads. As shown in Fig. 5(b), the power transfer capability is equal to the desired power of 300 W (30 kW at rated primary current 150 A) at rated load. Since the power transfer capability depends not only on the load resistance but also on the operational frequency, maximum power for bifurcation-free operation is achieved at a slightly higher load where the operational frequency is a little lower than the nominal frequency. This maximum power transfer capability is 322 W (32.2 kW at rated primary current 150 A).

With increasing load above the rated operation, the power transfer capability decreases rather than increases because the operational frequency drops away from the nominal frequency. In practice, control perturbations and transients affect the operational frequency of the variable-frequency controller in the bifurcation region. In order to investigate and measure the system operating at the three different ZPA frequencies and thereby verify the theory, the converter was made to operate in this region by increasing the load beyond the rated value while adjusting the turn-on interval of the inverter manually to force a shift between these operational frequencies. Under steady state conditions, the system was found to operate stably at either the lowest or highest ZPA frequency since perturbations that give a large positive phase angle will shift operation to the lowest ZPA frequency and perturbations that give a large negative phase angle will shift operation to the highest ZPA frequency.

As shown in Fig. 5, there is very good agreement between the measured and calculated operational frequency and power transfer. Small differences arise mainly from the violation of the theoretical assumption that the voltage and current are sinusoidal. In fact the inverter current is not strictly sinusoidal since some distortion of the voltage across the load impedance is unavoidable due to nonlinear switching control of the supply.

VI. Conclusion

Many practical ICPT systems are neither tightly nor loosely coupled. In such cases, coupling effects must be included in the system design to ensure phase or frequency shifts are minimized. In this paper, a new approach to the design of the primary compensation was presented that accounts for these coupling effects. The result is shown to be dependent on the secondary quality factor and the topology of the primary and secondary resonant circuits. This effect is more critical with parallel than series compensation. The proposed theoretical analysis and design considerations were confirmed using a contactless electric vehicle battery charger operating off a variable-frequency-controlled power supply.

References

[1] T. Bieler, M. Perrottet, V. Nguyen, and Y. Perriard, "Contactless power and information transmission," in *Conf. Rec. IEEE-IAS Annu. Meeting*, vol. 1, 2001, pp. 83–88.

[2] R. Laouamer, M. Brunello, J. P. Ferrieux, O. Normand, and N. Buchheit, "A multi-resonant converter for noncontact charging with electromagnetic coupling," in *Proc. IEEE IECON'97*, vol. 2, 1997, pp. 792–797.

[3] H. Abe, H. Sakamoto, and K. Harada, "A noncontact charger using a resonant converter with parallel capacitor of the secondary coil," *IEEE Trans. Ind. Appl.*, vol. 36, no. 2, pp. 444–451, Mar./Apr. 2000.

[4] Y. Jang and M. M. Jovanovic, "A contactless electrical energy transmission system for portable-telephone battery chargers," in *Conf. Rec. Telecommunications Energy Conf.*, 2000, pp. 726–732.

[5] G. B. Joun and B. H. Cho, "An energy transmission system for an artificial heart using leakage inductance compensation of transcutaneous transformer," *IEEE Trans. Power Electron.*, vol. 13, no. 6, pp. 1013–1022, Nov. 1998.

[6] A. Okuno, L. Gamage, and M. Nakaoka, "Performance evaluations of high-frequency inverter-linked DC/DC converter with noncontact pickup coil," *IEEE Trans. Ind. Electron.*, vol. 48, no. 2, pp. 475–477, Apr. 2001.

[7] J. T. Boys, G. A. Covic, and A. W. Green, "Stability and control of inductively coupled power transfer systems," *Proc. IEE—Elect. Power Appl.*, vol. 147, no. 1, pp. 37–43, Jan. 2000.

[8] G. A. Covic, G. Elliott, O. H. Stielau, R. M. Green, and J. T. Boys, "The design of a contact-less energy transfer system for a people mover system," in *Proc. Int. Conf. Power System Technology*, vol. 1, Dec. 2000, pp. 79–84.

[9] O. H. Stielau and G. A. Covic, "Design of loosely coupled inductive power transfer systems," in *Proc. Int. Conf. Power System Technology*, vol. 1, Dec. 2000, pp. 85–90.

[10] C.-S. Wang, G. A. Covic, and O. H. Stielau, "General stability criterions for zero phase angle controlled loosely coupled inductive power transfer systems," in *Proc. IEEE IECON'01*, vol. 2, 2001, pp. 1049–1054.

Chwei-Sen Wang received the B.E. degree in mechanical engineering from National Chiao Tung University, Hsinchu, Taiwan, R.O.C., the M.E. degree in mechanical engineering from National Taiwan University, Taipei, Taiwan, R.O.C., and the M.E. Hons. degree in electrical and electronic engineering from The University of Auckland, Auckland, New Zealand.

He is currently a Doctoral Fellow with the Foundation of Research, Science and Technology, New Zealand, while hosted in the Department of Electrical and Computer Engineering, The University of Auckland. He has been a Research Fellow in the Mechanical Industry Research Laboratory of the Industrial Technology Research Institute, Hsinchu, Taiwan, R.O.C., a Lecturer in the Department of Mechanical Engineering, National Chiao Tung University, and a Project Manager with Rechi Precision Company Ltd., Hsinchu, Taiwan, R.O.C. His research interests include automatic production systems, computer graphics, CAD/CAM, refrigerant compressors, room air conditioners, power electronics, and inductively coupled power transfer systems.

Oskar H. Stielau received the B.Eng., M.Eng., and D.Eng. degrees from Rand Afrikaans University, Johannesburg, South Africa, in 1986, 1988, and 1991 respectively.

He currently consults in the high-frequency power electronic field, specializing in inductive technologies. He is based in Auckland, New Zealand. Prior to this, he spent two years with the Inductive Power Transfer research group at The University of Auckland and seven years working in industry, mainly in the induction heating field.

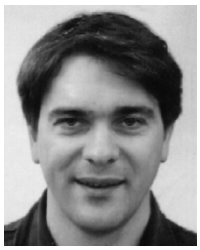

Grant A. Covic (M'88–SM'04) received the B.E. Hons. and Ph.D. degrees from The University of Auckland, Auckland, New Zealand, in 1986 and 1993, respectively.

He is a full-time Senior Lecturer in the Department of Electrical and Computer Engineering, The University of Auckland. His current research interests include power electronics, ac motor control, electric vehicle battery charging, and inductive power transfer. He has consulted widely to industry in these areas. He also has a strong interest in improved delivery methods for electronics and control teaching.